ECS Transactions, 66 (5) 243-250 (2015)
10.1149/06605.0243ecst ©The Electrochemical Society

Stress Considerations in Thin Films for CMOS-Integrated Gas Sensors

Lado Filipovic, Siegfried Selberherr

Institute for Microelectronics, TU Wien, Gußhausstraße 27-29/E360 Wien, Austria

The integration of gas sensing elements into hand-held electronics will provide individuals the ability to detect harmful chemicals and pollutants in the environment in real time. Metal oxide gas sensors rely on changes in their electrical conductance due to the interaction of the oxide with a surrounding gas at an elevated temperature. The intrinsic stress in the metal oxide films during the low-temperature, high-pressure, and low oxygen content sputter deposition of tin oxide (SnO_2) and indium-tin-oxide (ITO) is examined in this work. The surface free energy for the two films is found to be 1.69J/m^2 and 1.85J/m^2, respectively, and the intrinsic stress during the early stages of film growth is plotted. The spray pyrolysis deposition technique is implemented to grow a tin oxide film at 400ºC, which is able to detect the presence of multiple gases in the environment. Deposition at this temperature leads to a thermo-mechanical stress of 380MPa.

Introduction

The integration of gas sensor components into smart phones, tablets, and wrist watches will revolutionize the environmental health and safety industry by providing individuals the ability to detect harmful chemicals and pollutants in the environment using always-on hand held or wearable devices. However, before this can be achieved, several challenges must be overcome (1),(2),(3). Until recently, available gas sensors relied on a bulky architecture whose manufacture was not compatible with that of a conventional CMOS process sequence (4). The integration with CMOS processing is essential in order to combine the sensor with MEMS and CMOS microelectronics, as shown in Fig. 1. The output from each sensor unit is passed through an amplifier to a multiplexer. The multiplexer output is then sent through a low pass filter (LPF) and an analog to digital converter (ADC) before the signal can be analyzed with a microcontroller (μC) and eventually displayed or stored (2). Several different elements are required in order to enable the simultaneous detection of multiple gases.

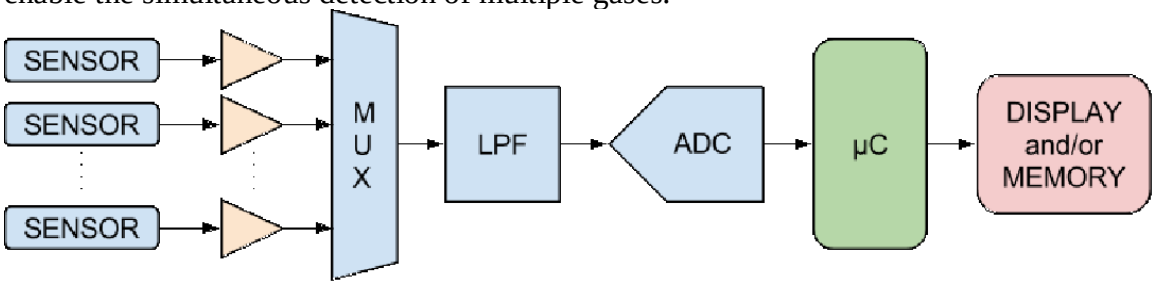

Fig. 1: Sensor array with interface electronics blocks. An array of multiple sensor elements is required in order to be able to independently sense a variety of gases.

Sensing Properties of Metal Oxide Thin Films

More recently, semiconducting metal oxides have been shown to exhibit very good conductometric sensing properties, when exposed to an ambient gas at high temperatures (5),(6). As already implied in Fig. 1 the operation of a smart gas sensor requires the ability to detect a multitude of hazardous gases in the environment, for which multiple sensor circuits are required. Metal oxide materials can be used as gas sensors, when heated to temperatures between 250ºC and 500ºC using a micro hot plate, as depicted in Fig. 2(a). At these temperatures oxygen is adsorbed at the metal oxide surface by trapping electrons from the bulk material, resulting in the band bending shown in Fig. 2(b). The overall result is a decrease or increase in the metal oxide resistance, depending on whether the material is n-type or p-type, respectively. The introduction of a target gas in the atmosphere causes a reaction with the surface oxygen, removing it from the interface and reducing the band bending effect and thereby the overall resistance (7), represented by the thin lines in Fig. 2(b).

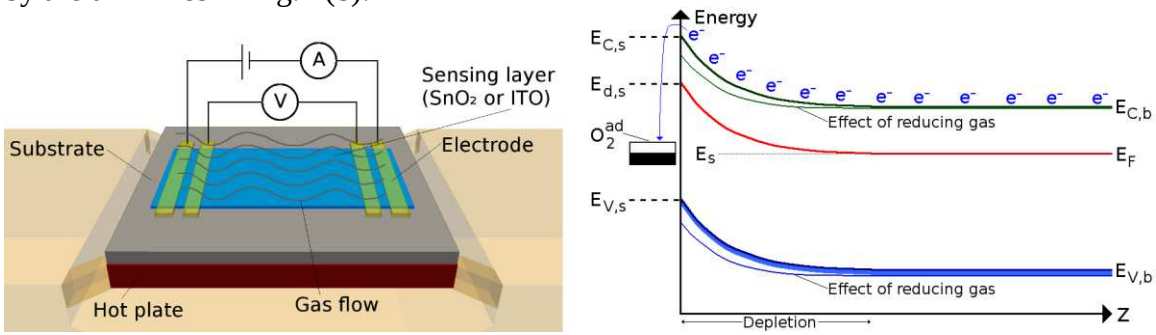

(a) Gas sensor schematic (b) Band bending

Fig. 2: (a) Principle view of the gas sensor on a micro hotplate, which is heated up to 250ºC-500ºC during sensor operation. (b) Schematic representation of the band bending effect caused by oxygen adsorption and subsequent introduction of a reducing gas.

The generation of the depletion layer through the interaction of oxygen and a reactive gas with the metal oxide film is depicted in Fig. 3. The thickness of the depletion layer is in the order of the Debye length, defined by

$$\lambda_D = \sqrt{(\varepsilon_0 * k_B * T) / (q^2 * n_c)}, \quad [1]$$

where ε_0 is the free space permittivity, k_B is the Boltzmann constant, T is the temperature, q is the elementary charge, and n_c is the carrier charge density.

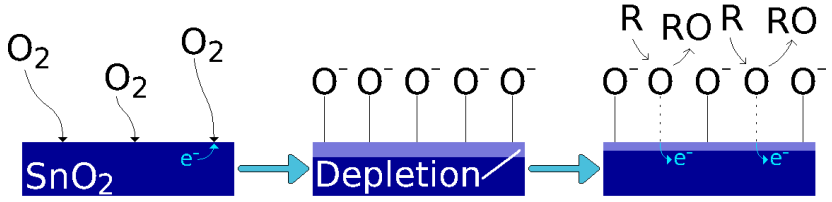

Fig. 3: Gas sensing function for a compact tin oxide film. The reaction occurs only at the top surface of the deposited tin oxide. The symbol R refers to a reducing gas.

The resistance of a metal oxide sensor is essentially comprised of the contact resistance R_c and two additional resistances occurring in parallel: (1) Surface resistance R_s, which is influenced by the surface reaction and (2) bulk resistance R_b, which is related

to the conductivity of the bulk metal oxide material, as depicted in Fig. 4. The resistance from the surface reaction changes depending on the ambient temperature and exposure to a reactive gas in the ambient, while the bulk resistivity and contact resistance stay constant (8). This study concerns itself with the stress generation in thin tin oxide (SnO_2) and tin-doped indium oxide (In_2O_3), known as indium-tin-oxide (ITO) thin films, because they have previously shown their usefulness as detectors for potentially dangerous and harmful gases including ethanol (C_2H_5OH) (9), acetone ($(CH_3)_2CO$) (9), nitrogen dioxide (NO_2) (9), carbon monoxide (CO) (10),(11), and hydrogen (H_2) (12). Acetone and ethanol belong to a group of organic chemicals referred to as volatile organic compounds (VOCs), which have a high vapor pressure at room temperature and often mix with interfering gases (13). Nitrogen dioxide is a combustible gas which can cause various problems in the environment such as smog and acid rain. NO_2 sensors are particularly important in automotive and truck applications. Carbon monoxide is a colorless, odorless, and tasteless gas which is toxic, when inhaled in high quantities, and CO poisoning is a common type of fatal air poisoning in many countries (14). The sensing of H_2 is essential in the design of smoke detectors.

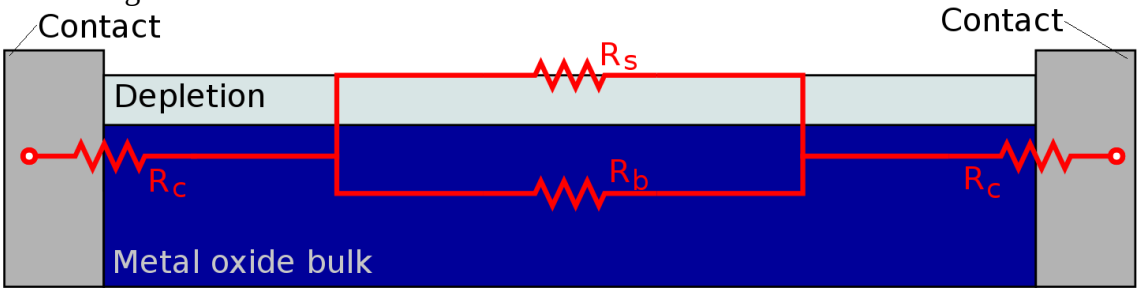

Fig. 4: Resistances acting during the operation of a metal oxide gas sensor. The surface resistance R_s is the only one which varies in the presence of a reactive gas.

Stress Generation During Metal Oxide Deposition

During metal oxide deposition a stress builds up which has a negative effect on the device reliability. The post-processing stress in a thin film is a result of two stress components: the intrinsic stress, which arises during the film growth, and the thermo-mechanical stress, which is a result of the difference in the deposition temperature and the subsequent cooling to room temperature. The thermo-mechanical stress is a concern, when high temperatures are used for the metal oxide deposition due to the difference in the coefficients of thermal expansion (CTE) between the depositing material and the silicon substrate. The growth mode of thin films depends on the surface free energy of the deposit, the substrate, and the interface between the two materials. The stress evolution during the deposition of tin oxide and indium-tin-oxide, is analyzed here. The growth process during sputtering is characterized by the Volmer-Weber growth mode (15), where small islands of the depositing film form on the surface which through expansion impinge on each other, eventually forming a coalesced thin film. Due to the surface interaction between the materials and the impingement of the depositing islands, a stress forms in the thin film (16). Although many metal oxides have shown a gas response in their conductivity, tin oxide and ITO have garnered particular attention. Due to the need for these films to be heated to temperatures between 250ºC and 500ºC during operation to increase the sensitivity, a considerable degradation of the film can result. In this study the post-processing stress through thin SnO_2 and ITO films is analyzed in order to obtain more information about the reliability of these metal oxides for operation in a gas sensor.

Intrinsic Stress during Metal Oxide Sputter Deposition

During the growth of metals and metal oxides on oxidized silicon surfaces, the film deposits in the form of islands which grow into grains. The initial stage of film deposition is island nucleation or the formation of small islands on the oxide surface, represented in Fig. 5(a). The islands then grow and impinge on each other (Fig. 5(b)), thereby generating tensile stress in the islands. When all islands are connected and the surface is covered with the metal oxide material, the film is said to coalesce, as shown in Fig. 5(c). The next stage of growth is film thickening, which can take two forms, either columnar or polycrystalline. The columnar thickening mode shown in Fig. 5(d) refers to the growth of films which have a high adatom mobility or low melting temperatures; the polycrystalline growth shown in Fig. 5(e) refers to the growth of films which have a low adatom mobility or high melting temperatures.

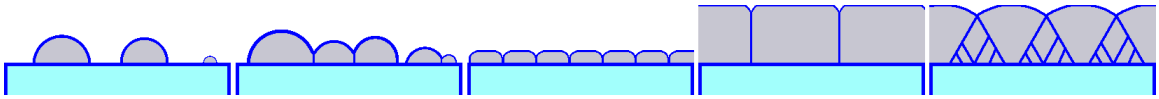

(a) Nucleation (b) Impingement (c) Coalescence (d) Thickening-I (e) Thickening-II

Fig. 5: Steps during film formation using the Volmer-Weber growth mode.

The evolution of the stress during film growth for the two types of materials is shown in Fig. 6(a). The generation of compressive stresses during nucleation and thickening as well as the generation of a tensile stress during coalescence is depicted. Fig. 6(b) shows the main cause for the presence of tensile stress. Two islands grow until they impinge on each other, preventing further radial expansion. Upon island impingement a grain boundary is formed between the islands, resulting in an energy reduction, as a part of the free surface of each island is eliminated. The process, referred to as "zipping" (16), generates tensile stress in each island and results in the islands forming grains with a grain boundary of height z_0. The generated tensile stress depends on the resulting geometry of the process, given in (16) as

$$\sigma_{tensile} = ½ * E/(1 - r^2) * (y_0 / r)^{1.3892}, \quad [2]$$

where E is the Young modulus, while r and y_0 are island-dependent geometric parameters shown in Fig. 6(b). Depending on the process parameters during the deposition of the metal oxides, the intrinsic stress in the film can be compressive (17),(18) or tensile (18),(19). The evolution of compressive stress during nucleation and thickening depends on the material's surface stress and the island geometry, given in (16) as

$$\sigma_{compressive} = - 2f / r * \sin\theta / [(1 - \cos\theta) * (2 + \cos\theta)], \quad [3]$$

where $f = \gamma_{gb} - 2\gamma_s$ is the surface free energy (γ_{gb} is the grain boundary energy and γ_s is the surface energy), r is the island radius, and θ is the contact angle between the island surface and the substrate, as shown in Fig. 6(b). This work deals with the tensile intrinsic stresses of sputtered SnO_2 and ITO. The SnO_2 is deposited at approximately 70ºC with a total pressure of 1.3Pa (18), while ITO is deposited at 50ºC in a high pressure environment of 3Pa (19).

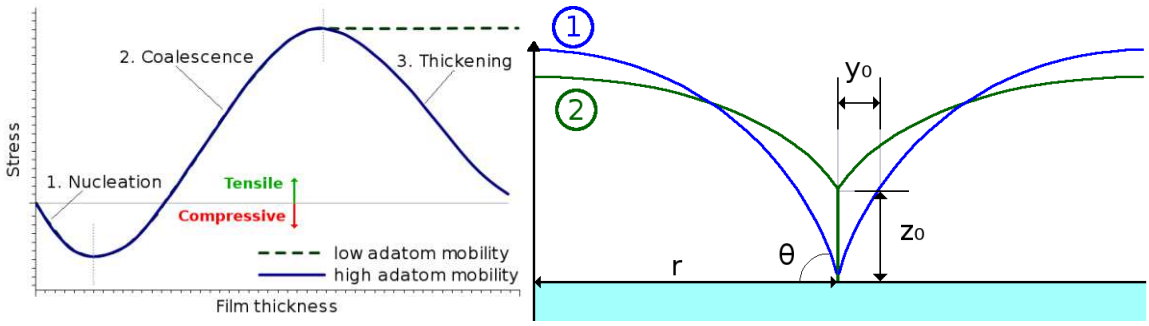

(a) Stress evolution during film growth (b) Two islands impinging on each other

Fig. 6: Stress development during the growth of a metal oxide film (a) as it changes between compressive and tensile at various stages of growth and (b) the geometry of two islands impinging on each other as they attempt to grow from position 1 to position 2, resulting in zipping and the creation of a grain boundary with height z_0.

Stress during Tin Oxide Sputter Deposition

During the sputter deposition of a 300nm-thick tin oxide film at approximately 70ºC and a low oxygen content in the sputtering gas, the stress is found to be 200MPa (18). When the oxygen content in the chamber is increased, the stress becomes more compressive. In this study the intrinsic stress formation in the tin oxide film during sputter deposition with a low oxygen content in the sputtering gas is examined. Knowing the expected intrinsic stress, the stress development during film growth can be analyzed using [2] and [3]. In Fig. 7 the growth of the intrinsic stress during the early stages of film growth can be seen. The stress starts compressive due to island nucleation and then becomes tensile during island impingement, reaching its maximum level of 200MPa at a thickness of about 50nm.

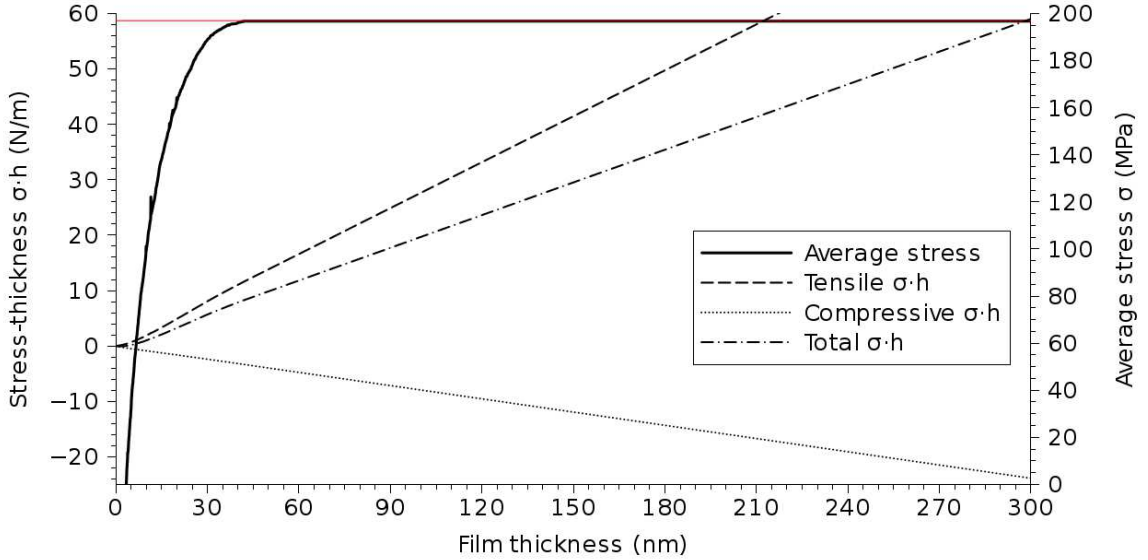

Fig. 7: Intrinsic stress generation during sputter deposition of tin oxide thin films at 70ºC. The stress-thickness is used to accurately observe the stress before film coalescence.

In addition to the average intrinsic stress through the deposited film, Fig. 7 shows how the stress builds up in the early stages of deposition, during island nucleation and

island impingement, prior to full film coalescence. During this time, the average stress is difficult to estimate as it shows a very low negative value, or a very high compressive stress. However, instead of showing the average stress, when the stress-thickness parameter ($\sigma \cdot h$) is plotted, the situation becomes more clear. The compressive and tensile stress components are tracked from the early stages of film growth. Using the parameters given in Table I and performing the intrinsic stress simulation during film growth, a value of 1.69J/m^2 for the surface free energy of the tin oxide film is found.

Stress during Indium-Tin-Oxide Sputter Deposition

During the sputter deposition of a 100nm-thick indium-tin-oxide film at approximately 50ºC and high atmospheric pressure in the ambient, the stress is found to be 300MPa (19). Decreasing the chamber pressure results in the stress turning more compressive, up to 2GPa, when a pressure below 1Pa is used (19). Knowing the expected tensile stress, the stress growth during film deposition can be analyzed using [2] and [3], as shown in Fig. 8. Using the parameters shown in Table I, a surface free energy of 1.85J/m^2 is calculated for the sputter deposited ITO film.

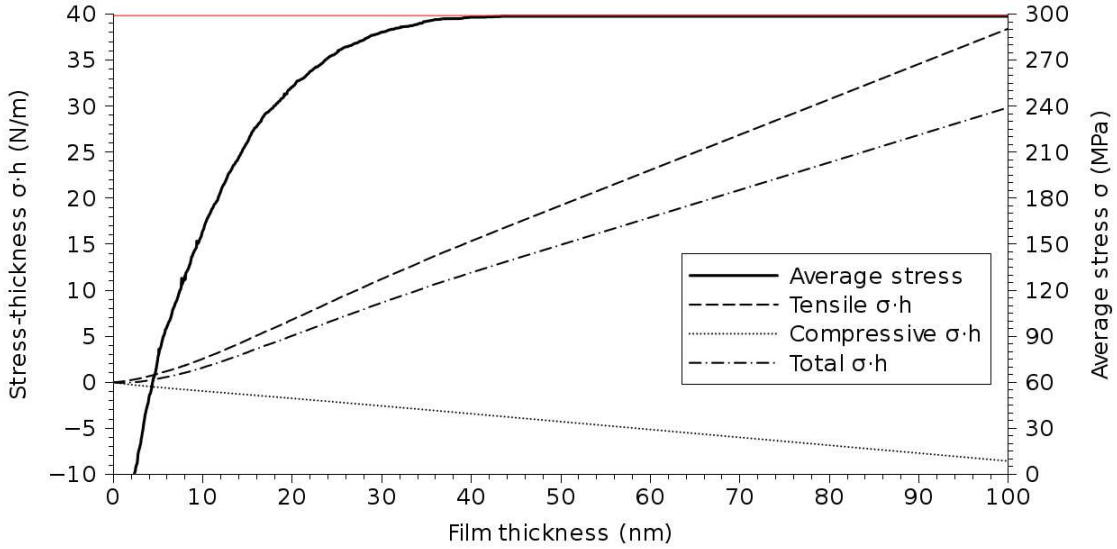

Fig. 8: Intrinsic stress generation during sputter deposition of ITO thin films at 50ºC.

TABLE I. Material properties of metal oxides SnO_2 and ITO required for the simulation of stress evolution. The values for the Young's modulus, Poisson's ratio, CTE, density, average grain size, and melting point are found in literature, while the values for the surface free energy and the contact angle between the island surface and substrate were found during this study.

Characteristic	**SnO_2**	**ITO**
Young's modulus E (GPa)	253 (20)	116 (21)
Poisson's ratio ν	0.293 (20)	0.33 (22)
CTE α (K^{-1})	4.0 x 10^{-6} (23)	8.5 x 10^{-6} (24)
Density ρ (g/cm^3)	6.99 (23)	7.18 (25)
Average grain size D (nm)	15 (26)	15 (27)
Melting point (ºC)	1900 (23)	1913 (25)
Intrinsic stress σ_i (MPa)	200 (18)	300 (19)
Surface free energy f (J/m^2)	1.69	1.85
Contact angle θ (º)	80	80
Thermo-mechanical stress σ_{th} (MPa)	50	35

Thermo-Mechanical Stress of Sputtered Films

The thermo-mechanical stress develops in films when a temperature difference is applied. In the case of metal oxide deposition, the stress arises after a thermal deposition step and the subsequent cooling to room temperature. For the sputter deposition processes for tin oxide and ITO, which are performed at 70ºC and 50ºC, respectively, the thermo-mechanical stress after cooling to room temperature is not significant. The tin oxide develops an additional 50MPa of tensile stress, while the ITO film develops an added 35MPa. However, when a thermal processing technique is used for the deposition of the thin film, the thermo-mechanical stress component has significantly more influence on the overall stress. This is further examined in the following section, where a thin SnO_2 film is deposited using the spray pyrolysis technique at 400ºC.

Spray Pyrolysis Deposition of Tin Oxide

The deposition of SnO_2 has been performed using a variety of techniques (28). The spray pyrolysis technique has gained traction over alternatives due to its cost effectiveness and ease of integration in the standard CMOS process. During deposition, a gas pressure nozzle is used to atomize a $SnCl_4$ + H_2O solution. The nozzle generates very small droplets which are directed towards the substrate, where SnO_2 is deposited on top of a heated wafer, as shown in Fig. 9. Using this method, substrates with complex geometries can be coated using CMOS-compatible temperatures at and below 400ºC. The nozzle is placed about 30cm away from the substrate, ensuring that the droplets have no horizontal velocity when reaching the vicinity of the substrate. The long distance between nozzle and wafer also ensures that all large, liquid droplets will be eliminated prior to reaching the substrate, ensuring a proper uniformity in the droplet size distribution and thereby a uniformity in the deposited film. A model for the deposition of thin films using this technique is presented in more detail in (4).

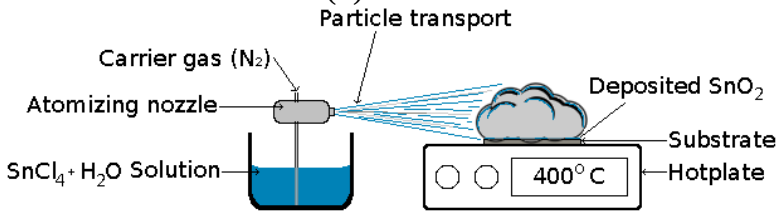

Fig. 9: Schematic of the experimental spray pyrolysis deposition process as set up for SnO_2 deposition with the wafer heated to about 400ºC.

Stress and Operation of Tin Oxide Deposited with Spray Pyrolysis

Because the tin oxide film is deposited at a temperature of 400ºC, the subsequent cooling to room temperature is expected to result in significantly more stress than that noted in the sputtered films. Using finite element simulations, the thermo-mechanical stress is found to be 380MPa, which is slightly higher than the intrinsic and thermo-mechanical stresses of the sputter-deposited films. However, this process technique allows us to affordably deposit a very thin 50nm film which is highly sensitive to several harmful gases. The ability to improve sensor performance by reducing the film thickness has already been proven in (29). With our process a 50nm thick film can be deposited on complex geometries with a 30 second spray burst of the $SnCl_4$ + H_2O solution. This film is able to detect CO, H_2, CO_2, CH_4, SO_2, H_2S, and other potentially harmful gases (30).

Summary and Conclusion

During the deposition of metal oxide films, which are essential for novel smart gas sensor devices, two stress components must be examined. One is the intrinsic stress which builds up during film growth through island nucleation, coalescence, grain formation, and film thickening. The second is the thermo-mechanical stress which is caused by the cooling of a deposited layer from a high processing temperature to room temperature. Sputtering, when performed at low temperatures results in films where the intrinsic stress is a major concern. However, when spray pyrolysis deposition is employed, the thermo-mechanical stress is more prominent because of the high temperature requirement during spray pyrolysis. The free surface energies of SnO_2 and ITO are found to be $1.69J/m^2$ and $1.85J/m^2$, respectively, and the intrinsic stress is analyzed during the early stages of deposition. The thermo-mechanical stress for spray pyrolysis-deposited SnO_2 at 400ºC is found to be 380MPa using finite element simulations.

References

1. I. Simon et al., *Sensor. Actuat. B-Chem.*, **73**(1), 1 (2001).
2. J. W. Gardner et al., *IEEE Sens. J.*, **10**(12), 1833 (2010).
3. C. Pijolat, in *Chemical sensors and biosensors/2012*, R. Lalauze, Editor, p. 93, John Wiley & Sons, Inc., Hoboken, NJ (2012).
4. L. Filipovic et al., *IEEE Trans. Semicond. Manuf.*, **27**(2), 269 (2014).
5. H. Meixner and U. Lampe, *Sensor. Actuat. B-Chem.*, **33**(1), 198 (1996).
6. C. Wang et al., *Sensors*, **10**(3), 2088 (2010).
7. N. Barsan and U. Weimar, in *Proc. 14th International Meeting on Chemical Sensors – IMCS 2012*, p. 618 (2012).
8. G. Chabanis et al., *Meas. Sci. Technol.*, **14**(1), 76 (2003).
9. Z. Jiao et al., *Sensor. Actuat. B-Chem.*, **94**(2), 216 (2003).
10. M. Di Giulio et al., *Sensor. Actuat. B-Chem.*, **23**(2), 193 (1995).
11. L Mädler et al., *J. Nanopart. Res.*, **8**(6), 783 (2006).
12. G. Mutinati et al., *Procedia Eng.*, **47**, 490 (2012).
13. N. Patel et al., *Sensor. Actuat. B-Chem.*, **96**(1) 180 (2003).
14. S. T. Omaye, *Toxicology*, **180**(2), 139 (2002).
15. M. Pletea et al., *J. Phys. Condens. Matter*, **21**(22), 225008 (2009).
16. S. C. Seel, *Stress and structure evolution during Volmer-Weber growth of thin films*, PhD thesis, Massachusetts Institute of Technology (2002).
17. Y. Vygranenko et al. *Phys. Status Solidi A*, **205**(8), 1925 (2008).
18. J. Boltz et al., *Surf. Coat. Technol.*, **205**(7), 2455 (2010).
19. T. Sasabayashi et al., *Thin Solid Films*, **445**(2), 219 (2003).
20. G. Gladysz and K. Chawla, *Compos. Part A-Appl. S.*, **32**(2), 778 (2001).
21. D. Neerinck and T. Vink, *Thin Solid Films*, **278**(1), 12 (1996).
22. T. Wittkowski et al., *Thin Solid Films*, **398-399**, 465 (2001).
23. M. Batzill and U. Diebold, *Prog. Surf. Sci.*, **79**(2), 47 (2005).
24. X. Guo et al., U. S. Patent 8,124,254 (2012).
25. A. Narazaki et al., *Appl. Phys. Express*, **6**(9), 92601 (2013).
26. D. D. Vuong et al., *Sensor. Actuat. B-Chem.*, **103**(1), 386 (2004).
27. A. Kulkarni et al., *Thin Solid Films*, **345**(2), 273 (1999).
28. D. Perednis and L. Gauckler, *Solid State Ionics*, **166**(3), 224 (2004).
29. V. Brinzari et al., *Thin Solid Films*, **391**(2), 167 (2001).
30. E. Brunet et al., *Sensor. Actuat. B-Chem.*, **165**(1), 110 (2012).